

Ion/Molecule Reactions of Cation Radicals Formed from Protonated Polypeptides via Gas-Phase Ion/Ion Electron Transfer

Yu Xia, Paul A. Chrisman, Sharon J. Pitteri, David E. Erickson, and Scott A. McLuckey*

Contribution from the Department of Chemistry, Purdue University, West Lafayette, Indiana 47907-2084

Received May 9, 2006; E-mail: mcluckey@purdue.edu

Abstract: Cation radicals formed via gas-phase electron transfer to multiply protonated polypeptides have been found to react with molecular oxygen. Such cation radicals are of interest within the context of electron transfer dissociation, a phenomenon with high utility for the characterization of peptide and protein primary structures. Most of the cation radicals show the attachment of O₂ under room temperature storage conditions in an electrodynamic ion trap. At higher temperatures and under conditions of collisional activation, the oxygen adduct species lose O₂, HO[•], or HO₂[•], depending upon the identity of the side chain at the radical site. The fragments containing the C-terminus, the so-called z-ions, which are predominantly radical species, engage in reactions with molecular oxygen. This allows for the facile distinction between z-ions and their complementary even-electron c-ion counterparts. Such a capability has utility in protein identification and characterization via mass spectrometry. Intact electron transfer products also show oxygen attachment. Subsequent activation of such adducts show dissociation behavior very similar to that noted for z-ion adducts. These observations indicate that ion/radical reactions can be used to probe the locations of radical sites in the undissociated electron transfer products as well as distinguish between c- and z-type ions.

Introduction

Within the past decade, significant attention has been placed on electron capture by gaseous multiply protonated proteins and peptides due to the structurally informative fragmentation that often results. The overall process has been termed electron capture dissociation (ECD),¹ and it provides a means for deriving structural information that complements, and often exceeds, that obtained via conventional ion activation techniques. It has recently been demonstrated that ion/ion electron transfer gives rise to dissociation behavior very similar to that noted from electron capture.² In the case of electron transfer dissociation (ETD), as well as in ECD, the major structurally informative dissociation channels give rise to complementary c- and z-type ions that are formed via cleavage of N–C α bonds of the amide backbone. Capture or transfer of an electron to an even-electron polypeptide cation creates an odd-electron species. Upon fragmentation, in the most common case, the c-product ion is

observed as an even-electron species and is denoted as a c' ion. The complementary z-type fragments, denoted as z[•], are odd-electron species with the radical site generally indicated to be located on the alpha-carbon of the cleaved bond. The charges of the ions associated with these products arise from one or more excess protons, and the presence of excess protons is usually implied in the labeling of a fragment as, for example, z_xⁿ⁺, where x denotes the location of the peptide cleavage and n denotes the magnitude of the charge as well as the number of excess protons when n > 1.

The formation of an odd-electron species from an even-electron polypeptide gives rise to radical chemistry that can play a role in the subsequent unimolecular behavior of the ion. For example, multiply protonated cyclic peptides have been shown to undergo extensive secondary side-chain and backbone fragmentation following electron capture³ that has been interpreted as being free-radical driven. Radical migration in long-lived electron capture products has also been demonstrated in deuterium labeled linear peptides.⁴ In this report, we demonstrate the ion/molecule reactivity that reflects the radical character of product ions formed via electron transfer. We have noted that molecular oxygen can attach to ions produced via ion/ion electron transfer and that this phenomenon is consistent with a radical mediated process. Reactions of molecular oxygen with

- (1) (a) Zubarev, R. A.; Kelleher, N. L.; McLafferty, F. W. *J. Am. Chem. Soc.* **1998**, *120*, 3265–3266. (b) Zubarev, R. A.; Kruger, N. A.; Fridricksson, E. K.; Lewis, M. A.; Horn, D. M.; Carpenter, B. K.; McLafferty, F. W. *J. Am. Chem. Soc.* **1999**, *121*, 2857–2862. (c) Zubarev, R. A.; Horn, D. M.; Fridricksson, E. K.; Kelleher, N. L.; Kruger, N. A.; Lewis, M. A.; Carpenter, B. K.; McLafferty, F. W. *Anal. Chem.* **2000**, *72*, 563–573. (d) Zubarev, R. A. *Mass Spectrom. Rev.* **2003**, *22*, 57–77.
- (2) (a) Syka, J. E. P.; Coon, J. J.; Schroeder, M. J.; Shabanowitz, J.; Hunt, D. F. *Proc. Natl. Acad. Sci. U.S.A.* **2004**, *101*, 9528–9533. (b) Coon, J. J.; Syka, J. E. P.; Schwartz, J. C.; Shabanowitz, J.; Hunt, D. F. *Int. J. Mass Spectrom.* **2004**, *236*, 33–42. (c) Pitteri, S. J.; Chrisman, P. A.; Hogan, J. M.; McLuckey, S. A. *Anal. Chem.* **2005**, *77*, 1831–1839. (d) Gunawardena, H. P.; He, M.; Chrisman, P. A.; Pitteri, S. J.; Hogan, J. M.; Hodges, B. D. M.; McLuckey, S. A. *J. Am. Chem. Soc.* **2005**, *127*, 12627–12639.

- (3) Leymarie, N.; Costello, C. E.; O'Connor, P. B. *J. Am. Chem. Soc.* **2003**, *125*, 8949–8958.
- (4) O'Connor, P. B.; Lin, C.; Cournoyer, J. J.; Pittman, J. L.; Belyayev, M.; Budnik, B. A. *J. Am. Soc. Mass Spectrom.* **2006**, *17*, 576–585.

relatively small gaseous alkyl radicals are known to give rise to alkyl peroxy radicals of relevance to atmospheric oxidation and hydrocarbon combustion.⁵ Peptide radical reactivity is well-established in the condensed phase,⁶ and protein ions have been shown to undergo gas-phase oxidation in a corona discharge.⁷ In the latter case, however, attack by hydroxyl radicals produced in the discharge was implicated as initiating the ion-radical reactions, which differs from the electron transfer or electron capture initiation steps relevant to ETD and ECD, respectively. The reactivity observed here has relevance to the possibility of using ion/molecule chemistry as a probe for radical site location in electron transfer and electron capture products, as well as for rapid distinction between N-terminal and C-terminal fragments formed from ETD and ECD. The latter application would be of particular utility in the role of gas-phase ion chemistry in modern high-throughput proteomics.

Experimental Section

Materials. Peptide samples were synthesized by SynPep (Dublin, CA). Acetic acid and methanol were obtained from Mallinckrodt (Phillipsburg, NJ). Nitrobenzene, azobenzene, and 1,3-dinitrobenzene were purchased from Sigma-Aldrich (St. Louis, MO). All peptide samples were used without further purification. Solutions of peptides were dissolved to 5 μM in a 50/50/1 (v/v/v) methanol/water/acetic acid solution.

Procedures. Most experiments were performed on a QqTOF tandem mass spectrometer (QSTAR XL, Applied Biosystems/MDS SCIEX, Concord, ON, Canada) modified to allow for ion/ion reaction studies.⁸ The instrument consisted of three quadrupoles (ion guide Q0, mass filter Q1, collision cell Q2) and a reflectron time-of-flight (TOF) analyzer with an orthogonal injection of ions.⁹ A home-built pulsed nano-electrospray (ESI)/atmospheric pressure chemical ionization (APCI) dual source¹⁰ was coupled directly to the nanospray interface of the QSTAR instrument. This dual source was comprised of a nano-ESI emitter for the formation of positive peptides ions ($(M + nH)^{n+}$) and an APCI needle for the formation of radical anions from the electron transfer reagents. Electron transfer ion/ion reactions were implemented in the Q2 linear ion trap (LIT) via superposing auxiliary radio frequency (rf) signals (80 kHz, 150 V) on the end lenses of the Q2 LIT to enable mutual storage of ions of opposite polarity. The pressure in Q2 LIT was adjustable in the range 2–12 mTorr with nitrogen as a bath gas. Oxygen was also employed in some cases as a bath gas to evaluate the ion–molecule reactivity of the products generated from electron transfer ion/ion reactions. The experimental sequence of electron transfer ion/ion reactions typically consisted of the following steps: anion injection to Q2 LIT (200 ms), positive ion injection to Q2 LIT (50 ms), and mutual cation/anion storage (100 ms). In some cases, subsequent ion isolation and collision-induced dissociation (CID) steps were applied to the electron transfer reaction products of interest. Ion isolation steps were achieved by the rf isolation ramps tuned to eject ions from selected ranges of mass-to-charge ratio.¹¹ CID was performed by resonantly exciting ions of interest (~ 200 ms) using a dipolar rf signal applied across one set of opposing rods of the Q2 quadrupole array. The final

products were analyzed by the reflectron TOF mass analyzer (20–50 ms), which offered a mass resolution of 6000–8000 and mass accuracy of ~ 50 ppm for external calibration. The TOF mass spectra shown here were typically the averages of 50–200 individual scans.

Heated electron transfer ion/ion reaction experiments were performed on a Hitachi (San Jose, CA) M-8000 3-DQ ion trap mass spectrometer modified for ion/ion reactions.¹² Peptide cations were formed using nano-ESI and entered the ion trap through an end cap electrode. Nitrobenzene radical anions were formed using an atmospheric sampling glow discharge ionization (ASGDI) source¹³ and were injected into the ion trap through a hole in the ring electrode. The order of events used in electron transfer ion/ion reaction experiments was very similar to those described above. The instrument's end cap heaters were controlled by a home-built external temperature controller. The heaters were set at a nominal temperature of 150 $^{\circ}\text{C}$, resulting in a helium bath gas temperature of 160–165 $^{\circ}\text{C}$ calibrated based on the thermal dissociation rate of +3 bradykinin ions.¹⁴

Results and Discussion

Much of the phenomenology noted from analysis of the charged products formed via electron transfer to a multiply protonated peptide and stored in an electrodynamic ion trap is reflected in the data displayed in Figure 1, which compares spectra collected for the reaction of triply protonated KGAILK-GAILR with azobenzene radical anions. Figure 1a shows data collected with nitrogen admitted to the LIT at a pressure of 5 mTorr, and Figure 1b shows the data collected when oxygen is admitted to the LIT at the same pressure and storage times. Note that oxygen is also present in the LIT for the experiment reflected in Figure 1a from the vacuum/atmosphere interface and from possible air contamination of the nitrogen. The peaks labeled z_x^* correspond to $(z_x^* + O_2)^+$, and for the z_1 – z_5 and z_7 – z_9 fragments, the z_x^*/z_x^* ratios clearly increase markedly when O_2 is used as the background gas in the LIT. There is also evidence in the O_2 experiment for the formation of z_6^* and z_{10}^* ions, although their abundances are quite small. However, the main species associated with these fragments change largely from z^* in the data acquired at low O_2 pressure (Figure 1a) to $(z^* - H^*)$ ions at the higher O_2 pressure (Figure 1b). It is noteworthy that $(z^* - H^*)$ ions are very rarely observed in either ETD or ECD.¹⁵ The most commonly observed even-electron z -ion, denoted as z' , corresponds formally to a $(z^* + H^*)$ species. Evidence given below suggests that the observation of $(z^* - H^*)$ ions in this instance is related to the dissociation of an intermediate z^* species by loss of HO_2^* . Use of variable reaction times, various O_2 pressures, different electron-transfer reagents (observation of O_2 adducts was independent of reagent anion), and accurate mass measurements (measured $z^* - z'$ mass difference = 31.9901 Da; O_2 mass = 31.9898 Da) implicated oxygen as being responsible for the formation of z^* species. Evidence for O_2 attachment to dozens of z^* ions subjected to storage conditions of room temperature and high O_2 pressure (up to 10 mtorr) has been noted. The observation of z^* species has also been made with a three-dimensional quadrupole ion trap and with a hybrid triple quadrupole/linear

- (5) (a) Wallington, T. J.; Dagaut, P.; Kurylo, M. J. *Chem. Rev.* **1992**, *92*, 667–710. (b) Finlayson-Pitts, B. J.; Pitts, J. N., Jr. *Atmospheric Chemistry*; Wiley: New York, 1986.
- (6) Barratt, B. J. W.; Easton, C. J.; Henry, D. J.; Li, I. H. W.; Radom, L.; Simpson, J. S. *J. Am. Chem. Soc.* **2004**, *126*, 13306–13311.
- (7) Frey, B. L.; Lin, Y.; Westphall, M. S.; Smith, L. M. *J. Am. Soc. Mass Spectrom.* **2005**, *16*, 1876–1887.
- (8) Xia, Y.; Chrisman, P. A.; Erickson, D. E.; Liu, J.; Liang, X.; Londry, F. A.; Yang, M. J.; McLuckey, S. A. *Anal. Chem.* **2006**, *78*, 4146–4154.
- (9) Shevchenko, A.; Chermushevich, I.; Ens, W.; Standing, K. G.; Thomson, B.; Wilm, M.; Mann, M. *Rapid Commun. Mass Spectrom.* **1997**, *11*, 1015–1024.
- (10) Liang, X.; Xia, Y.; McLuckey, S. A. *Anal. Chem.* **2006**, *78*, 3208–3212.
- (11) McLuckey, S. A.; Goeringer, D. E.; Glish, G. L. *J. Am. Soc. Mass Spectrom.* **1991**, *2*, 11–21.

- (12) (a) Reid, G. E.; Wells, J. M.; Badman, E. R.; McLuckey, S. A. *Int. J. Mass Spectrom.* **2003**, *222*, 243–258. (b) Pitteri, S. J.; Chrisman, P. A.; McLuckey, S. A. *Anal. Chem.* **2005**, *77*, 5662–5669.
- (13) McLuckey, S. A.; Glish, G. L.; Asano, K. G.; Grant, B. C. *Anal. Chem.* **1988**, *60*, 2220–2227.
- (14) Butcher, D. J.; Asano, K. G.; Goeringer, D. E.; McLuckey, S. A. *J. Phys. Chem. A* **1999**, *103*, 8664–8671.
- (15) Mirgorodskaya, E.; Roepstorff, P.; Zubarev, R. A. *Anal. Chem.* **1999**, *71*, 4431–4436.

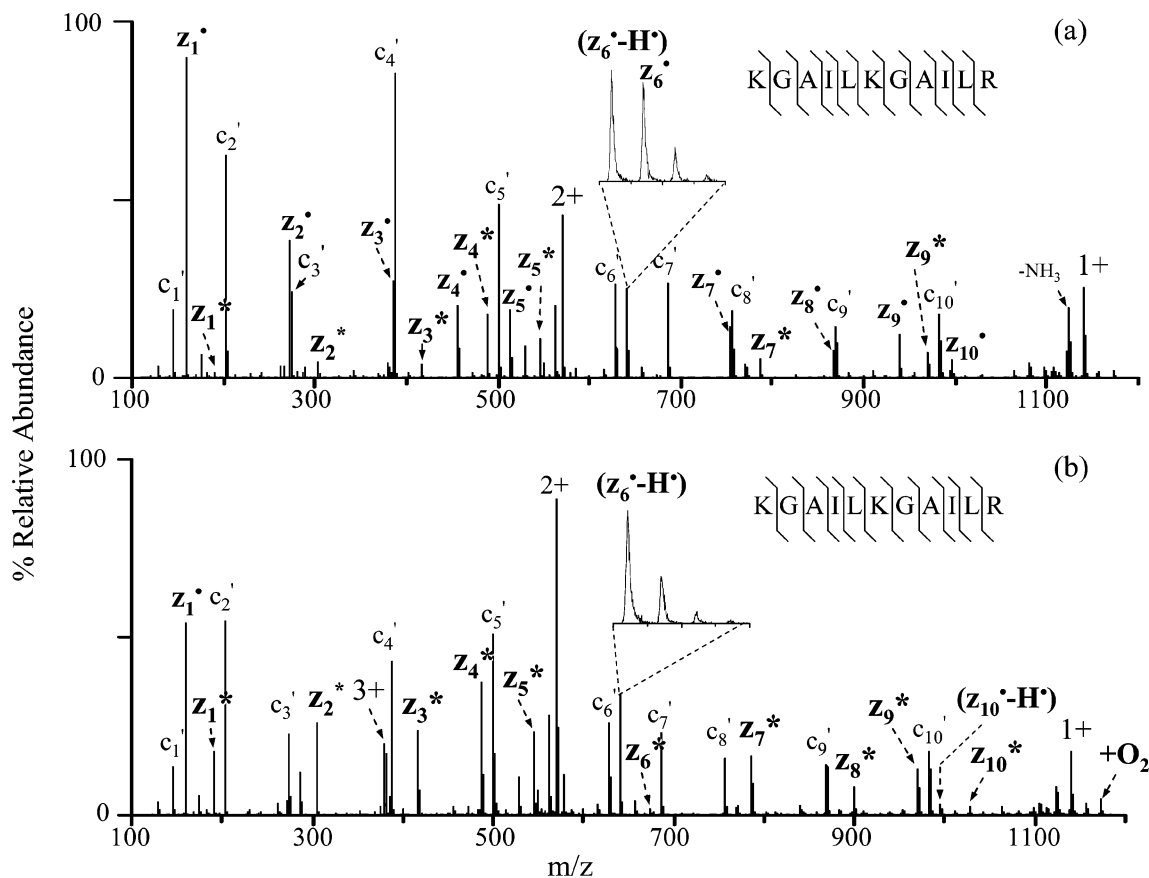


Figure 1. Mass spectra acquired after the reaction of $(M + 3H)^{3+}$ KGAILKGAILR with azobenzene radical anions for 100 ms in a linear ion trap charged with 5 mTorr nitrogen with a trace of oxygen (a) and charged with 5 mTorr of O_2 (b).

ion trap instrument, indicating the general nature of the phenomenon. No clear evidence for attachment of O_2 to c-type radical ions has thus far been noted, although this may be due to the minimal formation of c^* ions.^{1c}

The generality of z^* ion/oxygen reactivity has been tested with the ETD fragments generated from various peptides. Under conditions in which room temperature oxygen was added to the bath gas, evidence for formation of the z^* ion, usually via direct observation or sometimes via the observation of $(z^* - HO^*)$ or $(z^* - H^*)$ ions, was apparent for every single z^* species regardless the nature of their amino acid compositions. Such an example can be found in Figure 2, where melittin, a 26-residue polypeptide, has been subjected to electron transfer reactions for 100 ms with oxygen (5 mtorr) as the bath gas. The formation of z^* adduct ions is clearly seen for almost all z ions formed from ETD, while all z ions show evidence for at least one of the oxygen-related reaction products (viz., z^* , $(z^* - HO^*)$, and/or $(z^* - H^*)$ ions, as summarized in Figure 2d). No oxygen adducts were found for any of the c species.

MS^3 experiments involving z^* ions have been performed to shed further light on the reaction of O_2 with z^* ions. Figure 3, for example, compares the collision-induced dissociation of the z_1^* (Figure 3a) and z_1^* (Figure 3b) ions of KGAILKGAILR. The major dissociation products of the z_1^* ion are cations that contain a portion of the arginine side chain. A product of lesser abundance is also observed that corresponds to a loss of C_3H_4 (the only plausible combination of atoms from this precursor ion that falls within the mass tolerance of the measurement), which clearly must occur via a rearrangement process. In the

case of the z_1^* ion, loss of O_2 to yield the z_1^* ion and loss of HO_2^* to yield the $(z_1^* - H^*)$ ion are major dissociation channels. Other fragments in common with those of the z_1^* ion are also present in the data for the z_1^* ion, and these may well result from sequential fragmentation.

A third major loss channel noted from z^* ions is illustrated in the data of Figure 4, which shows CID data from the z_3^* (Figure 4a) and z_4^* (Figure 4b) ions derived from ETD of triply protonated KGAILKGAILR. In the case of the z_3^* precursor ion, fragmentation is dominated by loss of the hydroxyl radical (the mass measurement accuracy of the reflectron TOF allows for the ready distinction between loss of HO^* (17.0027 Da) and loss of NH_3 (17.0265 Da)). In this case, very little loss of O_2 or HO_2^* is observed. Relatively small signals are also observed that apparently arise from fragmentation reactions that involve rearrangements leading to side-chain loss. One such product is consistent with the label $(z_3^* - C_3H_7O_2^*)$, although the label is not intended to imply that the mechanism first involves formation of the z_3^* ion followed by loss of $C_3H_7^*$. For example, the same nominal product can also arise from loss of C_3H_6O from the $(z_3^* - HO^*)$ ion. In the case of the CID of the z_4^* ion, the loss of the hydroxyl radical is observed, although to a lesser degree than the loss of O_2 , which is the most abundant process, and the loss of HO_2^* . A variety of lower mass products are also observed that can arise either from sequential fragmentation reactions or directly from the precursor. The labels associated with the products are provided to indicate the nominal identities, but the labels themselves are not intended to imply that MS^4 experiments have been conducted to establish genealogy.

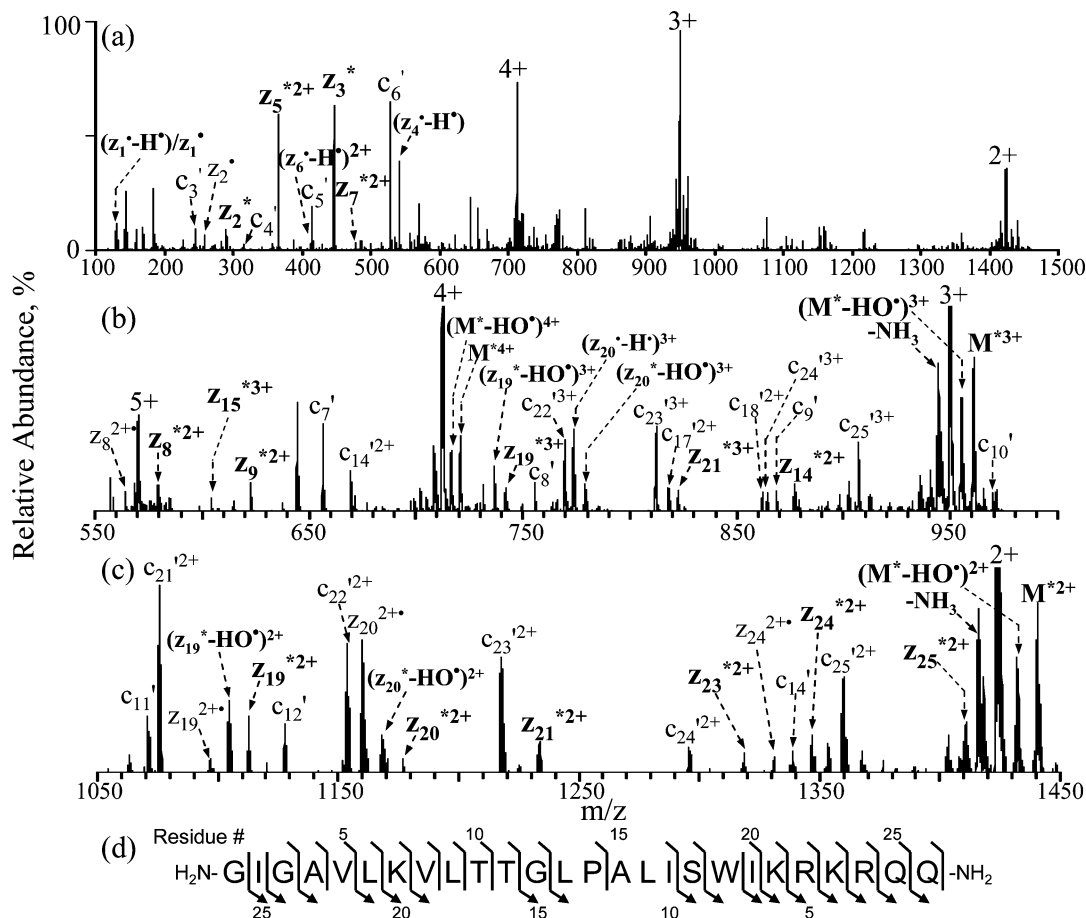


Figure 2. (a) Mass spectrum acquired after the reaction of $(M + 5H)^{5+}$ melittin with azobenzene radical anions for 100 ms in a linear ion trap charged with 5 mTorr oxygen. The zoomed m/z regions of (a) are shown in (b) and (c). $(M + nH + O_2)^{(n-1)+}$ ions are denoted as $M^{*(n-1)+}$. (d) The resulting backbone cleavages of melittin from ETD with the arrow sign indicating an observation of z^* formation at the indicated residue.

The data of Figures 3 and 4 are shown here primarily to illustrate the three major first generation dissociation channels noted for z^* ions; viz., O_2 loss, HO^\bullet loss, and HO_2^\bullet loss. Scheme 1 is provided to show mechanisms that can contribute to each of the major losses from z^* ions.

The major variables that determine the relative contributions of these competitive dissociation channels have not been delineated thus far. Clearly, the identity of the side chain attached to the carbon formally indicated as the radical site in the z^* ion can be expected to play an important role. However, contributions from nearest neighbor and conformational effects cannot be precluded at this point. The possibility for hydrogen migration in long-lived electron transfer products, as recently indicated in long-lived electron capture products,⁴ may also play a role in the MS^3 experiments as the ions subjected to CID have lifetimes on the order of at least tens of milliseconds.

It has been noted that signals arising from z^* adduct ions are greatly reduced when the gas in the ion trap is elevated above room temperature by roughly 100 K or more. Figure 5 shows a comparison between ETD experiments of $(M + 3H)^{3+}$ neurotensin collected on a three-dimensional-quadrupole ion trap with trace oxygen present in the bath gas when the bath gas was not actively heated ($\sim 25^\circ C$, Figure 5a) and when it was heated ($\sim 160^\circ C$, Figure 5b).

The obvious difference of Figure 5a and b is that while z^* adduct ions are clearly apparent under the lower temperature condition, they are almost absent in the data collected

when the trap is heated. The abundance of the M^* ion ($(M + nH + O_2)^{(n-1)+}$), which is the oxygen adduct of the undissociated electron transfer product, is also greatly decreased at the higher temperature, while an increase in relative abundance is noted for the $(M^* - HO^\bullet)$ ion. Note that while z^* ions are labeled in Figure 5, the corresponding $(z^* - H^\bullet)$ ions might also be formed. Due to the limited resolving power of the ion trap instrument, a distinction between these two products could not readily be made. Based on the tendency for many z^* ions to lose O_2 upon CID, the diminished abundances of z^* ions at higher bath gas pressures likely reflect a lower survival rate of z^* ions at the higher temperatures. Since the $(z^* - H^\bullet)$ ions, which are interpreted to arise from loss of HO_2^\bullet from z^* ions, are noted at room temperature, the abundances of the $(z^* - H^\bullet)$ ions are not adversely affected by elevating the bath gas temperature. In general, the $(z^* - HO^\bullet)$ ions are often observed to be more prominent at the higher bath gas temperatures.

Preliminary rate measurements were conducted for the formation of z^* ions derived from ETD of triply protonated KGAILKGAILR over reaction times of 30–200 ms at room temperature and an O_2 pressure of 5 mTorr. The reaction rates were determined from the slopes of plots of $-\ln[z_n^*]_t / ([z_n^*]_i + [z_n^*]_t)$ versus time, which fell within the range $0.6\text{--}6\text{ s}^{-1}$, depending on the identity of the z^* ion. Given the reversible nature of these reactions and the observed temperature dependence of z^* ion formation, further studies are warranted to

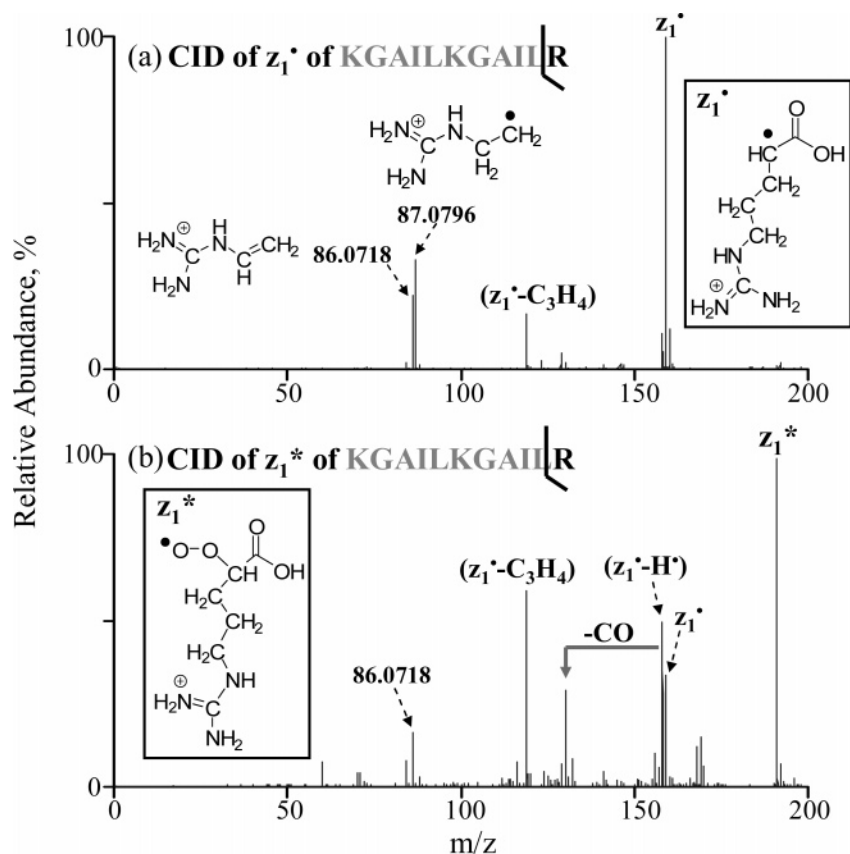


Figure 3. CID spectra of the (a) z_1^* and (b) z_1^* ions derived from ETD of $(M + 3H)^{3+}$ KGAILKGAILR.

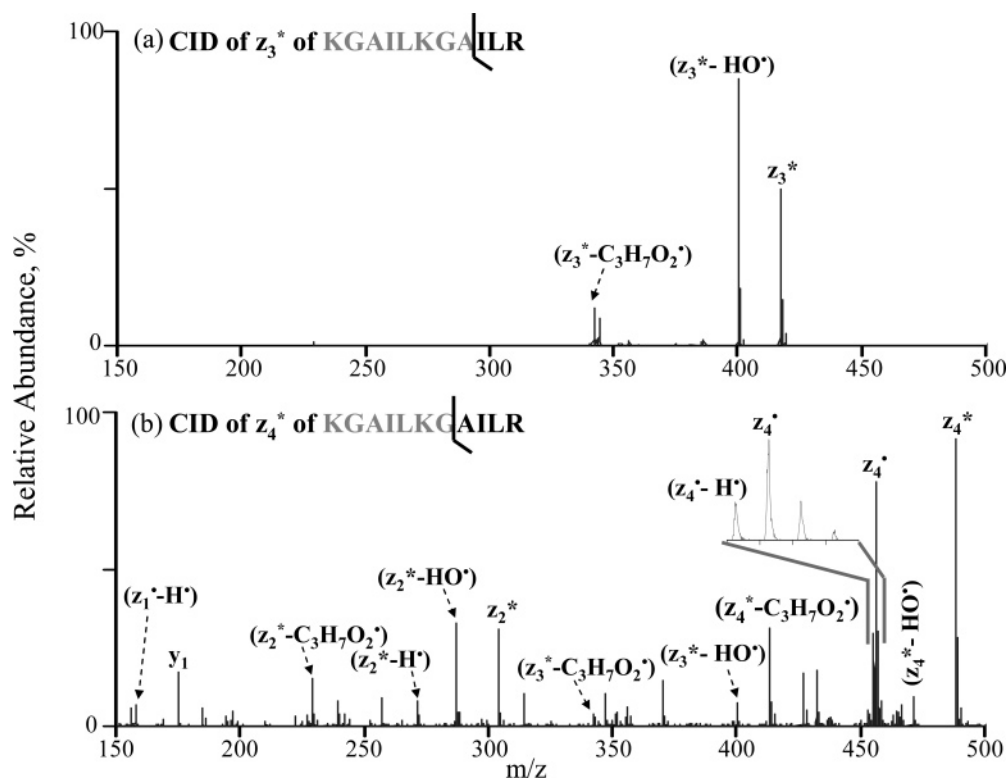


Figure 4. CID spectra of the (a) z_3^* and (b) z_4^* ions derived from ETD of $(M + 3H)^{3+}$ KGAILKGAILR.

determine the efficiencies of these reactions. If it is assumed that the reactions are irreversible under these experimental conditions, rate constants of $(4-40) \times 10^{-15} \text{ cm}^3 \text{ molecule}^{-1} \text{ s}^{-1}$ are obtained. These values must be regarded as lower limits,

however, given the possibility for adduct decomposition even at room temperature. The observation of some $(z^* - H^*)$ ions at room temperature suggests that decomposition of z^* ions can be significant even at relatively low bath gas temperatures.

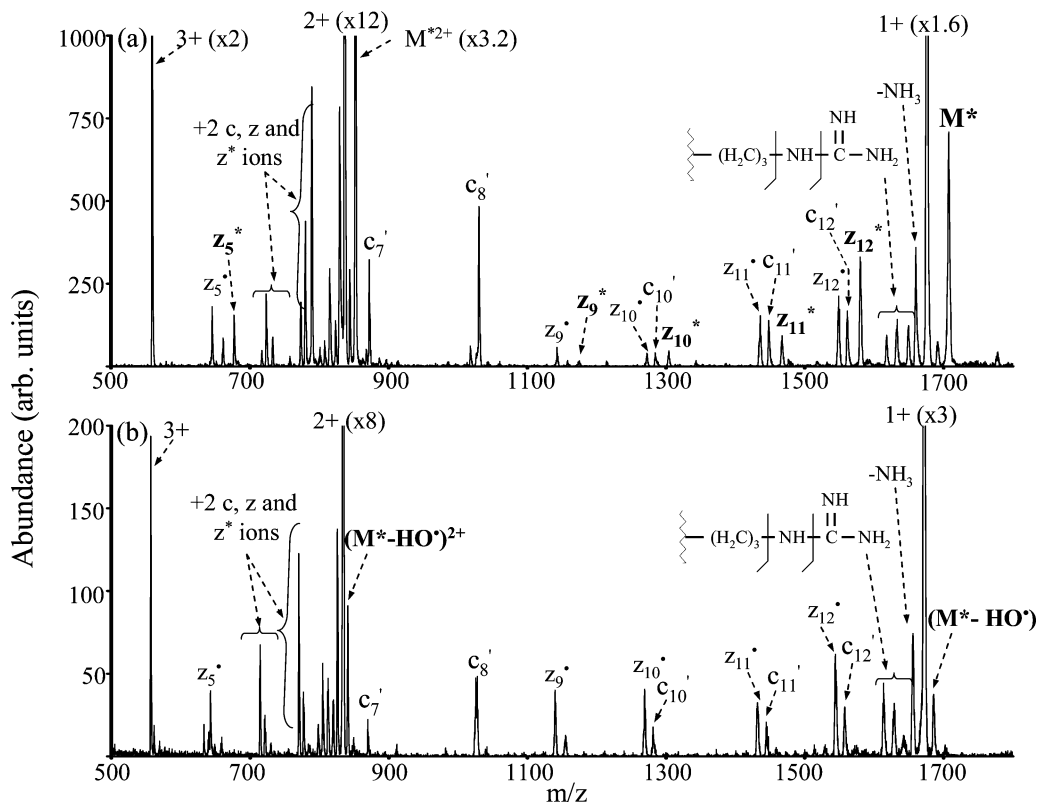
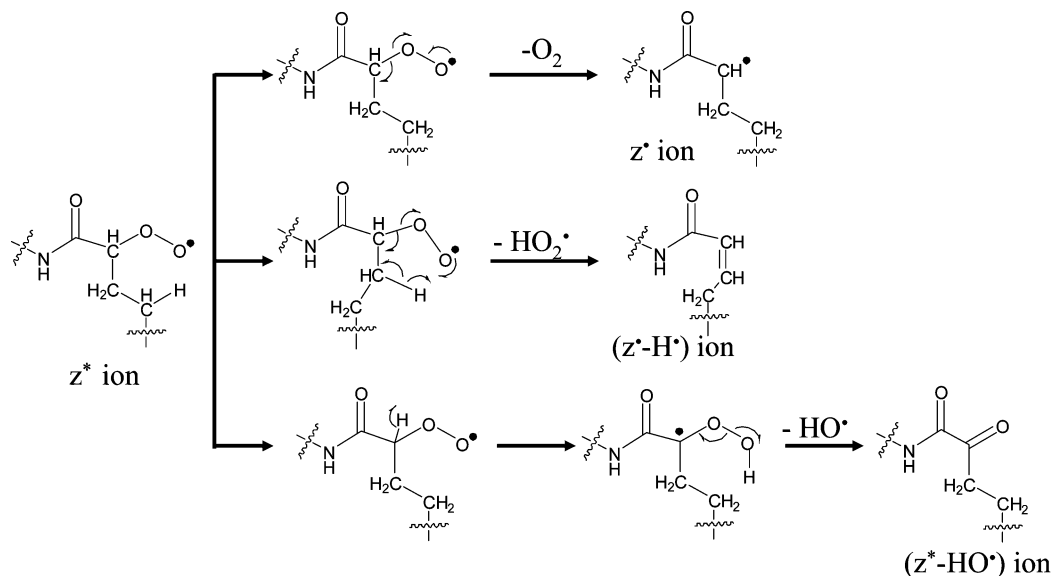


Figure 5. Mass spectra acquired after the reaction of $(M + 3H)^{3+}$ neurotensin with nitrobenzene radical anions in a quadrupole ion trap under (a) room temperature and (b) heated conditions ($\sim 160^\circ\text{C}$). The $(M + 2H + O_2)^{+}$ and $(M + 3H + O_2)^{2+}$ ions are denoted as M^* and M^{*2+} , respectively.

Scheme 1. Mechanisms Involving Amino Acid Side Chains that Can Give Rise to the Major Losses Noted in the CID of z^* Ions



Electron capture by or electron transfer to protonated polypeptides also often leads to the formation of radical-cation products of the form $(M + nH)^{(n-1)+\bullet}$ that do not produce dissociation products directly. Subsequent gentle activation of such products generally gives rise to either complementary c'/z^* or c^*/z' fragments. The latter complementary pair has been noted to be much more prevalent from long-lived $(M + nH)^{(n-1)+\bullet}$ ions than from those that fragment directly following electron capture or transfer.¹⁶ It can be argued that a covalent bond of the $(M + nH)^{(n-1)+\bullet}$ ion is cleaved but that noncovalent interactions prevent the separation of the products¹⁷ or that all

covalent bonds remain intact and that the subsequent activation is necessary to cleave peptide backbone bonds. In either case, the ion is an odd-electron species, and at least some of them react with O_2 , as reflected in Figure 6a, which shows the results of a 100 ms ion/ion reaction in 10 mTorr O_2 between triply protonated neurotensin and the azobenzene radical anion. Both

(16) Swaney, D. L.; McAlister, G. C.; Schwartz, J. C.; Suka, J. E. P.; Coon, J. J. Proceedings of the 54th ASMS Conference on Mass Spectrometry, Seattle, WA, May 28–June 1, 2006.

(17) Breuker, K.; Oh, K. B.; Horn, D. M.; Cerda, B. A.; McLafferty, F. W. *J. Am. Chem. Soc.* **2002**, *124*, 6407–6420.

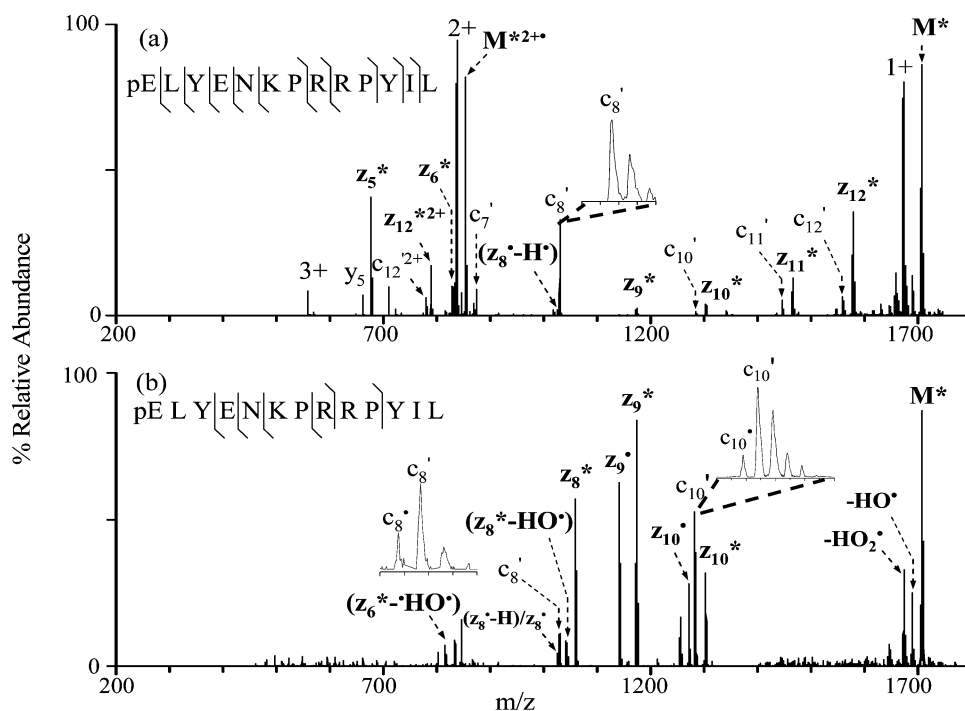


Figure 6. (a) Mass spectrum acquired after the reaction of $(M + 3H)^{3+}$ neurotensin with azobenzene radical anions for 100 ms in a linear ion trap charged with 10 mTorr O_2 and (b) the CID spectrum of the $(M + 2H + O_2)^{+}$ ion, denoted in the figure as M^* .

doubly and singly charged pseudo-molecular product ions show significant degrees of O_2 attachment, as do the z-type ions.

Figure 6b shows the product ion spectrum derived from ion trap collisional activation of the $(M + 2H + O_2)^{+}$ ions (M^* in the figure). Losses of HO_2^{\bullet} and HO^{\bullet} are each observed. Loss of O_2 is not particularly prominent, but such a loss presumably gives rise to a reactive species that can reattach oxygen. Several c- and z-related ions are also noted. Particularly prominent are z_8 , z_9 , and z_{10} related ions (i.e., z^* , z^* , $(z^* - H^{\bullet})$, and $(z^* - HO^{\bullet})$) with the abundances and types varying with z_x . Interestingly, the z-type ions most prominent in Figure 6b are of only minor abundance in Figure 6a. An interpretation consistent with this observation is that the population of ions that fragment in the experiment of Figure 6a differs in terms of the distribution of radical site locations from the ions sampled in the experiment of Figure 6b. It has already been noted that the collisional activation of electron transfer “survivor” peptide ions often gives rise to product ion spectra with quite different distributions of c- and z-products.^{2c} It may be significant that the dissociation behavior of the collisionally activated $(M + 2H + O_2)^{+}$ ion is very similar to that of the MS³ results of z^* ions. Such behavior is consistent with the hypothesis that amide bonds are already broken thereby creating the radical sites associated with z^* ions that can attach O_2 . However, the possibility that z^* ions are formed in conjunction with the collisional activation of an $(M + 2H + O_2)^{+}$ ion with initially intact amide bonds cannot be precluded.

Conclusions

The results reported here indicate that molecular oxygen reacts with cation radicals formed via electron transfer (and presumably via electron capture) to multiply protonated polypeptides. In the case of ETD products, the fact that the z-type ions are

predominantly formed as radical species permits the facile distinction between c-type and z-type ions. Such a capability could be useful in improving the confidence of identification of protein ions on the basis of matching product ion data with *in silico* predicted data. For a given ion/ion reaction time, the presence of oxygen in the ion/ion reaction volume at an appropriate level can yield both z_n^* and z_n^* ions. Doublets that differ in mass by 32 Da can be used to identify the z-type fragments. The dissociation behavior of z-ions with oxygen adducts can also apparently provide information about the environment of the radical site, although the factors that play the primary roles in determining the partitioning among loss of O_2 , loss of HO_2^{\bullet} , and loss of HO^{\bullet} require further study. Ion-radical/molecule reactions can also be used to probe the ions that do not yield obvious dissociation products. Dissociation of the oxygen adducts likely reflects the location of the radical sites in the formally intact polypeptide cation radicals. Advantage can be taken of such reactivity both for practical applications (e.g., proteomics) and to improve understanding of the nature of the products formed via electron transfer or capture.

Acknowledgment. Research supported by Chemical Sciences, Geosciences and Biosciences Division, Office of Basic Energy Sciences, Office of Sciences, U.S. Department of Energy, under Award No. DE-FG02-00ER15105 and the National Institutes of Health under Grant GM 45372. Y.X. acknowledges support from a Merck Research Laboratories Fellowship. MDS Sciex is acknowledged for its key role in adapting the instrument for ion/ion reaction studies. Dr. Richard A. J. O’Hair is acknowledged for helpful discussions. X. Liang is acknowledged for his help on the experiments on a hybrid triple quadrupole/linear ion trap instrument.

JA063248I